Real-Time Reconstruction of the Strong-Field-Driven Dipole Response

V. Stooß,[1] S. M. Cavaletto,[1] S. Donsa,[2] A. Blättermann,[1] P. Birk,[1]
C. H. Keitel,[1] I. Březinová,[2] J. Burgdörfer,[2] C. Ott,[1] and T. Pfeifer[1,*]
[1]*Max-Planck-Institut für Kernphysik, Saupfercheckweg 1, 69117 Heidelberg, Germany, EU*
[2]*Institute for Theoretical Physics, Vienna University of Technology, Wiedner Hauptstraße 8, 1040 Vienna, Austria, EU*

(Received 6 August 2018; published 26 October 2018)

The reconstruction of the full temporal dipole response of a strongly driven time-dependent system from a single absorption spectrum is demonstrated, only requiring that a sufficiently short pulse is employed to initialize the coherent excitation of the system. We apply this finding to the time-domain observation of Rabi cycling between doubly excited atomic states in the few-femtosecond regime. This allows us to pinpoint the breakdown of few-level quantum dynamics at the critical laser intensity near 2 TW/cm^2 in doubly excited helium. The present approach unlocks single-shot real-time-resolved signal reconstruction across timescales down to attoseconds for nonequilibrium states of matter. In contrast to conventional pump-probe schemes, there is no need for scanning time delays in order to access real-time information. The potential future applications of this technique range from testing fundamental quantum dynamics in strong fields to measuring and controlling ultrafast chemical and biological reaction processes when applied to traditional transient-absorption spectroscopy.

DOI: 10.1103/PhysRevLett.121.173005

The measurement of the fastest dynamical processes in nature typically relies on observing the nonlinear response of a system to precisely timed interactions with external stimuli [1,2]. This usually requires two (or more) controlled events, e.g., a triggering pump and a delayed probe pulse, with time-resolved information gained by controllably varying the interpulse delays. For example, femto- and attosecond time-resolved absorption spectroscopy [3–5] were used with great success to access explicitly time-dependent excited-state dynamics to uncover the nonequilibrium electron dynamics of atomic [6–8], molecular [9–11], and condensed-phase [12–14] systems in the presence of additional interactions. Such out-of-equilibrium processes include, e.g., the coupling of multielectron configuration channels [15], strong-field manipulation of autoionization [16,17], or the strong coupling between excited quantum states [18,19]. Thus, accessing and understanding the nonlinear response of such processes is of crucial importance for controlling and steering quantum dynamics on the attosecond timescale [20–25].

By measuring an absorption spectrum alone, causality has been used in the past to retrieve the complex linear response function [26–29]. Recent theoretical and experimental work [30–34] suggests a link between the shape of spectral lines and amplitude and phase shifts of the response function of the system. This has even been observed in the presence of strong nonlinear interactions which drive the observed system out of equilibrium, making it explicitly time dependent. Thus far, however, only the special case of a sudden modification of the response function was understood analytically, leaving the general case of the dynamical response to arbitrary interactions open to interpretation [35]. The question then arises: how can we temporally resolve the response of a system in the presence of an additional explicitly time-dependent nonlinear interaction from a single spectrum?

The absorption spectrum $A(\omega)$ or cross section $\sigma(\omega)$ is proportional to the Fourier transform of the dipole response function $d(t)$ caused by a weakly perturbing field $\varepsilon_\gamma(t)$ [36],

$$A(\omega) \propto \sigma(\omega) \propto \omega \,\mathrm{Im}\left(\frac{\mathcal{F}[d(t)]}{\mathcal{F}[\varepsilon_\gamma(t)]}\right) \quad \text{for } \omega > 0, \qquad (1)$$

where, in the linear regime, $\mathcal{F}[d(t)]$ is linearly proportional to $\mathcal{F}[\varepsilon_\gamma(t)]$. For time-translation-invariant systems, Eq. (1) has in the past frequently provided the starting point of a large number of probes of physical systems through their linear response. Under the condition of weak perturbations and utilizing the connection between amplitude (absorption) and phase (dispersion) owing to causality [26–29], the Fourier transform of the complete linear absorption spectrum corresponds to the response of a system to a (virtual) broadband excitation event. Thus, the spectrum carries

information about the system's internal structure (e.g., resonant excitations) including the natural decay dynamics on the characteristic timescale T_d. The decay times can be extracted for probing fields $\varepsilon_\gamma(t)$ with pulse duration T_γ much larger than the timescale of the system ($T_\gamma \gg T_d$), simply by tuning the laser frequency through the spectral linewidth. It is even possible to use an incoherent probe field $\varepsilon_\gamma(t)$, where the system interacts at random points in time with photons of various frequencies resolved by a spectrometer. This is because, for a time-translation-invariant system, the relative phases between frequency components and, subsequently, the arrival time of the probing photons are irrelevant. By contrast, the evolution of a general nonequilibrium state of matter cannot be accessed by incoherent fields, as the system can exhibit explicit time dependence.

In the more general case of a system subject to a time-dependent interaction $V(t)$, the response function becomes interaction and time dependent $d[V(t), t]$ (see Fig. 1 for an illustration). As a consequence, this explicitly time-dependent response can no longer be measured with incoherent light, i.e., photons arriving at random times. To solve this problem, consider the response to a coherent (laser) pulse $\varepsilon_\gamma(t)$, preceding an external perturbation $V(t)$. Let the duration T_γ of the pulse $\varepsilon_\gamma(t)$ be much shorter than the timescale T_V of $V(t)$ and decay time T_d of the system ($T_\gamma \ll T_V$, T_d). In this impulsive limit [formally approximated by $\varepsilon_\gamma(t) = \varepsilon_\gamma \delta(t)$, with the Dirac delta function $\delta(t)$], the absorption spectrum from Eq. (1) transforms into

$$A(\omega) \propto \mathrm{Im}\{\mathcal{F}[d(V(t), t)]\} \quad \text{for } \omega > 0. \tag{2}$$

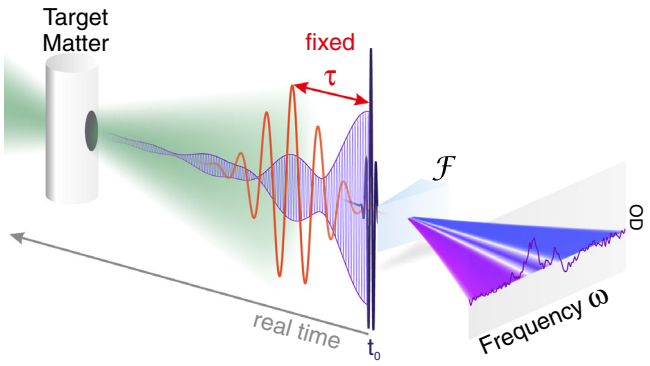

FIG. 1. Nonequilibrium response of matter: illustration of the probing of a nonequilibrium state of matter induced by a time-dependent perturbation $V(t)$ using ultrashort laser pulses (dark blue at t_0) to trigger a response (purple), which is then modified, e.g., by a strong external time-dependent electric field (red). From the measured absorption spectrum [Eq. (1)], the strongly driven response can be fully reconstructed if the initial excitation pulse is much shorter than the system's dynamics [Eq. (2)]. In this case, the initial excitation near $t_0 = 0$ produces a causal response, and the response can be reconstructed using the Fourier transform of the measured spectrum (see Supplemental Material, Sec. 3 [37]).

Because of causality [26–28], the real part $\mathrm{Re}\{\mathcal{F}[d(V(t), t)]\}$, and consequently the entire information on the coherent dipole $d[V(t), t]$ excited by the short pulse $\varepsilon_\gamma(t)$, can be reconstructed from Eq. (2) (see Supplemental Material, Sec. 3 [37]), to read

$$d(t) \propto \mathcal{F}^{-1}[iA(\omega)](t) = \frac{1}{2\pi}\int_{-\infty}^{+\infty} iA(\omega)e^{-i\omega t}d\omega \quad \text{for } t > 0, \tag{3}$$

where $A(\omega)$ is formally extended to negative frequencies by setting it to zero for $\omega < 0$. As a consequence, no second (probe) pulse is necessary to sample dynamical information. A single absorption spectrum suffices without the need for scanning a time delay. For the case of a linear response only, a similar approach was discussed in [29]. Here we show that for a strongly driven system under any interaction $V(t)$, beyond perturbation theory, the time-dependent response can be reconstructed.

For a proof-of-principle demonstration of the reconstruction method, we numerically calculate the response for the near-infrared (NIR) field-driven Rabi-cycling dynamics of doubly excited states in helium. As a first approach, we use a few-level model (see Supplemental Material, Sec. 2.2 [37]), composed of the $1s^2$ ground state and the $2s2p$ and $2p^2$ excited states. It includes the NIR coupling between the two excited states as well as their natural autoionization decay, while neglecting all other states or strong-field-induced ionization effects. The $2s2p$ state is initially coherently excited by a weak and broadband attosecond extreme ultraviolet (XUV) pulse (realizing the Dirac-delta-like excitation) and, subsequently, strongly coupled to the $2p^2$ state by the NIR pulse which interacts after an arbitrary but fixed time delay. The dipole response, driven and modified by a strong laser pulse at a time delay of 7 fs after the excitation, is shown in Fig. 2(a). The resulting absorption spectrum $A(\omega)$, calculated according to Eq. (1), is depicted in Fig. 2(b). In order to retrieve the real-time dipole response $d_{\mathrm{rec}}[V(t), t]$ near the $2s2p$ state, we apply a Gaussian window filter centered at 60.15 eV (FWHM of 4 eV indicated by green lines) and take the inverse Fourier transform. Figure 2(d) shows the reconstruction for a broader filter (orange lines). Given this broader bandwidth for the reconstruction, even the fast oscillations of $d_{\mathrm{rec}}[V(t), t]$ can be resolved. The near-perfect agreement between the reconstructed [Fig. 2(d)] and original directly calculated coherent dipole response [Fig. 2(a)], including the entire time-resolved holographic (amplitude and phase) information, confirms the validity of the approach for isolated resonances.

In the following, this reconstruction principle is experimentally applied to an important prototypical problem in strong-field atomic physics and attosecond science: the

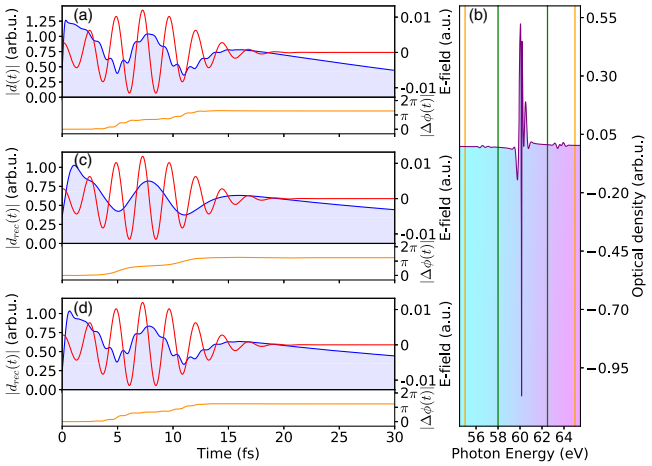

FIG. 2. Test of the reconstruction method: (a) Amplitude (blue curve) and phase induced by the NIR field (modulo 2π, orange curve) of the numerically simulated time-dependent response function using a few-level model including two excited states. The red curve shows the electric field of the nonlinearly interacting laser pulse. (b) Calculated optical density from (a) according to Eq. (1). (c) Test of the reconstruction method of amplitude and phase of the response function by selecting (Gaussian filter window with its FWHM indicated by green lines) the plotted spectral range and taking the inverse Fourier transform of the observable spectrum (b) restricted to the causal domain ($t \geq 0$). (d) Same as (c), using a broader filter window (orange lines). Here also the fast oscillations in the response can be reconstructed.

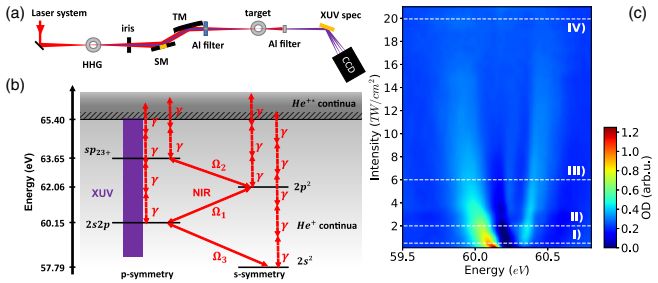

FIG. 3. Experimental setup and data: (a) Illustration of the experimental apparatus. High-harmonic generation neon gas target (HHG), split-mirror setup for setting the XUV-NIR time delay (SM), toroidal mirror (TM), XUV flat-field spectrometer (XUV spec). (b) Level scheme of the relevant doubly excited states of helium. The NIR pulse induces resonant couplings Ω_1, Ω_2, Ω_3 between the autoionizing doubly excited states and also leads to resonantly enhanced strong-field multiphoton ionization into the $N = 2$ continuum at the highest intensities of up to 20 TW/cm^2. (c) NIR intensity scan of Autler-Townes splitting [34] in doubly excited helium around the $2s2p$ state at 60.15 eV at fixed time delay $\tau = 7.4 \pm 0.1$ fs. The high spectrometer resolution allows the observation of the line shape in great detail. White dashed lines I–IV indicate the spectra used in the reconstruction discussed in Fig. 4.

strong coupling between correlated, autoionizing two-electron states [16,17] in an intense laser field. The experimental setup is displayed in Fig. 3(a), employing a typical attosecond transient-absorption beam line [32]. With this setup, we realize the pulse configuration illustrated in Fig. 1, where first the doubly excited states of helium [see Fig. 3(b)] are coherently excited by XUV attosecond-pulsed light defining the time $t_0 = 0$ for the measurement. The system then interacts with a sub-7-fs (full width at half maximum of intensity) NIR laser pulse after a fixed time delay of $\tau = 7.4 \pm 0.1$ fs. This delay was chosen such that the overlap between the NIR and the XUV pulse is minimized, and, most importantly, the NIR pulse now strongly drives the two-electron excited-state dynamics on a timescale (7 fs) prior to a significant depletion of the $2s2p$ state with a natural lifetime of 17 fs.

As an example, we now retrieve the intensity-dependent real-time-resolved dipole dynamics of the $2s2p$ autoionizing state. With increasing intensity, this resonance exhibits an Autler-Townes splitting [50], primarily due to the coupling with the $2p^2$ autoionizing state, as shown in Fig. 3(c). The results of the response reconstruction applied to these data are presented in Fig. 4 for a wide range of intensities. We reconstruct both the amplitude and the phase (blue lines) of the time-dependent dipole moment (TDDM) $d_{2s2p}(t)$. The reconstructed dipole response is compared with fully *ab initio* simulations (green lines), solving the time-dependent Schrödinger equation for helium in the presence of the XUV and NIR fields (see Supplemental Material, Sec. 2.1 [37]). In order to identify more clearly the contribution from individual states during the strong-field NIR excitation, we use a few-level model (see [37], Sec. 2.2), now including all states shown in Fig. 3(b), as well as autoionization and multiphoton ionization (orange lines). The results in Fig. 4 are normalized to the curves at zero NIR intensity.

The four NIR intensities represent different regimes of strong-field interaction from the weak perturbative regime to the regime of strong coupling and strong-field ionization of autoionizing states. For NIR intensities of $I_{\mathrm{NIR}} = 0.5$ and 2.0 TW/cm^2, the TDDM amplitude in Figs. 4(a) and 4(b) displays increasingly pronounced minima. For higher NIR intensities of $I_{\mathrm{NIR}} = 6.0$ TW/cm^2 and up to $I_{\mathrm{NIR}} = 20.0$ TW/cm^2[Figs. 4(c) and 4(d)], several temporal oscillations are observed with rapid phase changes near each minimum of the amplitude. The *ab initio* simulation allows for a direct and unambiguous determination of the full time-dependent dipole moment and confirms the reconstructed dipole response for this strongly driven helium system. Deviations at early (0–1 fs) and late times may result from the non-Gaussian experimental pulse shape and the experimental limitation of the measurement of spectrally very broad and low-signal line shapes, which would require very long measurement times and a more precise determination of the reference spectrum not possible with the current apparatus.

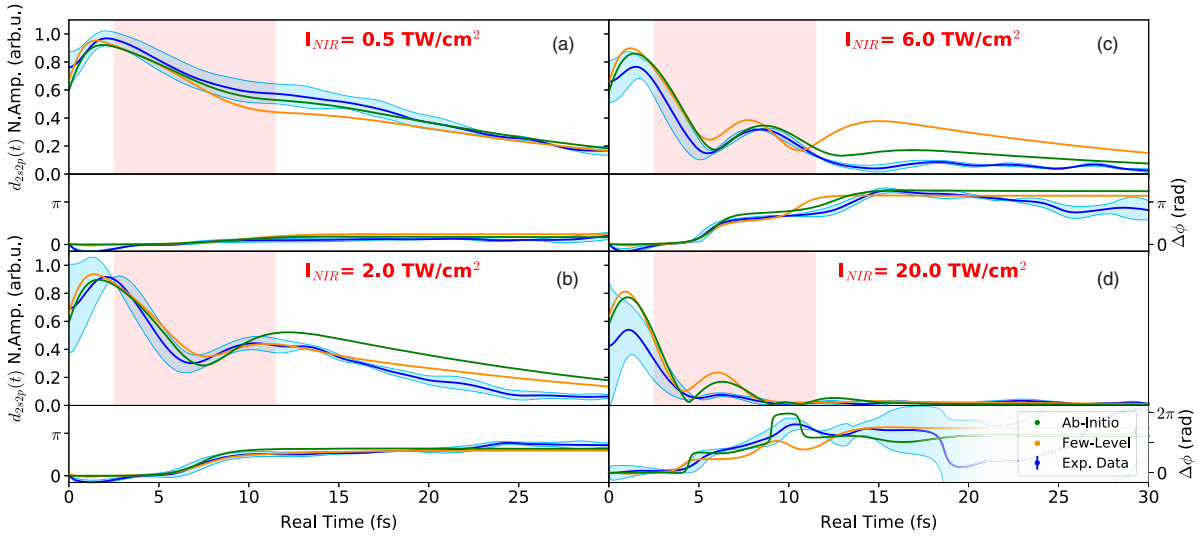

FIG. 4. TDDM $d_{2s2p}(t)$ of the doubly excited helium $2s2p$ state: (a),(b) Reconstructed TDDM amplitude and phase change (modulo 2π, blue), showing the emerging departure from the simple exponential decay during the interaction with the central part of the NIR pulse (red shaded area) for the intensities $I_{\mathrm{NIR}} = 0.5$, 2.0 TW/cm^2. (c),(d) The TDDM develops several minima and phase steps indicative of Rabi oscillations due to resonant coupling between the $2s2p$ and $2p^2$ states. The onset of strong-field ionization and the resulting depletion of the states during the NIR pulse for higher intensities at $I_{\mathrm{NIR}} = 6.0$, 20.0 TW/cm^2 is visible. The error bars (blue shaded area) show the standard deviations of the reconstructed time-dependent response. The orange curves show the calculated amplitude and phase evolution of the TDDMs using a few-level model, including configuration interaction V_{CI} pathways and multiphoton ionization, where the latter becomes increasingly important at the highest laser intensities. The green lines represent *ab initio* calculations.

The comparison between the few-level model and the *ab initio* calculation allows more detailed insights into the strong-field-driven coupling dynamics. For weak XUV excitations and subsequent interactions that leave the ground state unaffected, the dipole is directly related to the amplitude (and thus population) of the excited state. The minima in the amplitude combined with the associated phase changes therefore indicate a significant resonant population transfer due to Rabi oscillations mostly between the $2s2p$ and the $2p^2$ states. The increasing number of minima with increasing NIR intensity directly follows from the field dependence of the generalized Rabi frequency $\Omega_{R,ij} = \sqrt{\Delta_{ij}^2 + \Omega_{ij}^2(t)}$, with $\Omega_{ij}(t) = \varepsilon_{\mathrm{NIR}}(t) \cdot \mu_{ij}/\hbar$, where $\varepsilon_{\mathrm{NIR}}(t)$ is the NIR electric field, $\mu_{ij} = \langle i|\hat{\mu}|j\rangle$ is the transition dipole matrix element connecting two doubly excited states, and Δ_{ij} is the respective detuning of the laser from the transition frequency between states $|i\rangle$ and $|j\rangle$.

At higher intensities, the decrease in the TDDM amplitude as a function of time shows that the contributions of NIR-driven ionization can no longer be neglected. In the absence of an analytical model for nonlinear laser ionization of doubly excited states, we employ in the few-level model state-resolved ionization rates $\Gamma_n = \alpha_n I_{\mathrm{NIR}}(t)^n$, with $I_{\mathrm{NIR}}(t)$ being the time-dependent NIR intensity envelope, n is the order of the process (number of absorbed photons), and α_n are constants adjusted for each involved state but independent of intensity. The amplitude evolution of the TDDM predicted by this model still shows qualitative agreement with its experimentally reconstructed counterpart and the *ab initio* results at higher NIR intensities [Fig. 4(a)–4(c)].

From the phase evolution at highest intensity shown in Fig. 4(d), even the Rabi cycling to the $2s^2$ excited state [51–53], albeit not resonantly coupled, can be unambiguously detected by the phase change by about $-\pi$ near 10 fs, visible in both the experiment and *ab initio* calculation. This state plays a significant role in the strongly driven quasibound state dynamics and has to be accounted for explicitly in order to achieve agreement with the experimental results.

The TDDM approach allows one to explore the transition from few-level to complex multilevel coupling dynamics with increasing field strength. For both theory and experiment, Figs. 5(a) and 5(b) show the amplitude of the reconstructed response at real time $t = 7.5$ and 20 fs after the excitation, respectively. In both cases, the *ab initio* simulation agrees well with the experiment. The few-level model, however, starts to disagree significantly, not only quantitatively but also qualitatively, above an intensity threshold of about 2.0 TW/cm^2. Analysis of the *ab initio* simulation, shown in Fig. 5(c), provides an explanation: a rapid increase of dynamical complexity in a small quantum system. Above intensities of about 2.0 TW/cm^2, the number of states contributing to the dynamics increases abruptly, explaining the breakdown of the few-level model.

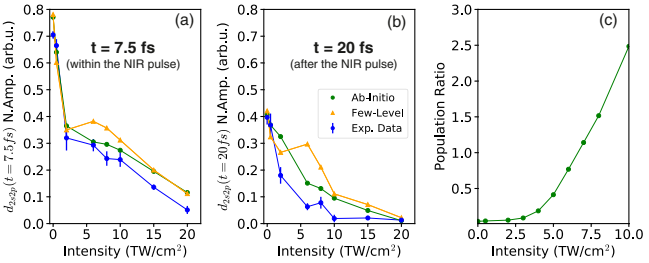

FIG. 5. The onset of complex strong-field dynamics in a small quantum system: (a) Amplitude of the reconstructed response at time $t = 7.5$ fs during the interaction with the NIR pulse (at time delay $\tau = 7.4$ fs). (b) Amplitude of the reconstructed response at real time $t = 20$ fs, i.e., after the interaction with the NIR pulse has concluded. The few-level model starts to significantly deviate from experiment and *ab initio* simulation between 2.0 and 6.0 TW/cm^2 (c) The population ratio between the population in 24 excited states excluding the four states used in the few-level simulation and the population in these four states after the strong-field interaction at $t = 20$ fs, extracted from the *ab initio* simulation. This explains the breakdown of the few-level model: an abrupt increase of the state space involved in the dynamics that sets in at intensities between 2.0 and 6.0 TW/cm^2. For even higher intensities, the interpretation in a few-state framework is no longer reliable.

Additionally, the *ab initio* simulation indicates that the assumption in the few-level model of neglecting ionization to the adjacent continua is no longer viable.

As the time-domain reconstruction approach described above in Eq. (3) makes no assumptions about the system under study [37], it is generally applicable, also to complex systems. For example, absorption bands in large molecules interacting with strong laser fields [54] could be analyzed in the time domain. Furthermore, the real-time reconstruction approach is viable for single-shot transmission spectra, which, for example, may emerge into a powerful new tool at short-wavelength free-electron lasers. Here, the nonlinear response could be used to uncover the *in situ* timing and ensuing dynamics of x-ray and optical pulses, which are otherwise often lost due to a temporal jitter. The underlying concept is not limited to the interaction with electric fields and can be more generally applied to the reconstruction of nonequilibrium response functions of any kind of interaction, in particular, to the magnetic dipole response, and across all spectral energy regions.

We acknowledge funding from the European Research Council (ERC) (X-MuSiC-616783). This work was supported by the WWTF through Project No. MA14-002, and the FWF through Projects No. FWF-SFB041-VICOM, No. FWF-SFB049-NEXTLite, No. FWF-W1243-Solids4Fun, as well as the IMPRS-APS. The calculations were performed on the Vienna Scientific Cluster (VSC).

*Corresponding author.
thomas.pfeifer@mpi-hd.mpg.de

[1] R. W. Boyd, *Nonlinear Optics*, 3rd ed. (Elsevier LTD, Oxford, 2008).
[2] P. Hamm and M. Zanni, *Concepts and Methods of 2D Infrared Spectroscopy* (Cambridge University Press, Cambridge, 2011).
[3] E. Goulielmakis *et al.*, Nature (London) **466**, 739 (2010).
[4] H. Wang, M. Chini, S. Chen, C.-H. Zhang, F. He, Y. Cheng, Y. Wu, U. Thumm, and Z. Chang, Phys. Rev. Lett. **105**, 143002 (2010).
[5] M. Holler, F. Schapper, L. Gallmann, and U. Keller, Phys. Rev. Lett. **106**, 123601 (2011).
[6] Z.-H. Loh, M. Khalil, R. E. Correa, R. Santra, C. Buth, and S. R. Leone, Phys. Rev. Lett. **98**, 143601 (2007).
[7] S. Chen, M. J. Bell, A. R. Beck, H. Mashiko, M. Wu, A. N. Pfeiffer, M. B. Gaarde, D. M. Neumark, S. R. Leone, and K. J. Schafer, Phys. Rev. A **86**, 063408 (2012).
[8] M. Chini, X. Wang, Y. Cheng, and Z. Chang, J. Phys. B **47**, 124009 (2014).
[9] E. Warrick, W. Cao, D. M. Neumark, and S. R. Leone, J. Phys. Chem. A **120**, 3165 (2016).
[10] C. T. Liao and A. Sandhu, Photonics **4**, 17 (2017).
[11] M. Reduzzi, J. Phys. B **49**, 065102 (2016).
[12] M. Schultze *et al.*, Science **346**, 1348 (2014).
[13] M. Lucchini, S. A. Sato, A. Ludwig, J. Herrmann, M. Volkov, L. Kasmi, Y. Shinohara, K. Yabana, L. Gallmann, and U. Keller, Science **353**, 916 (2016).
[14] M. Schultze *et al.*, Nature (London) **493**, 75 (2013).
[15] U. Fano, Phys. Rev. **124**, 1866 (1961).
[16] P. Lambropoulos and P. Zoller, Phys. Rev. A **24**, 379 (1981).
[17] H. Bachau, P. Lambropoulos, and R. Shakeshaft, Phys. Rev. A **34**, 4785 (1986).
[18] I. I. Rabi, S. Millman, P. Kusch, and J. R. Zacharias, Phys. Rev. **55**, 526 (1939).
[19] M. Chini, X. Wang, Y. Cheng, Y. Wu, D. Zhao, D. A. Telnov, S.-I. Chu, and Z. Chang, Sci. Rep. **3**, 1105 (2013).
[20] A. Assion, T. Baumert, M. Bergt, T. Brixner, B. Kiefer, V. Seyfried, M. Strehle, and G. Gerber, Science **282**, 919 (1998).
[21] S. Haessler *et al.*, Phys. Rev. X **4**, 021028 (2014).
[22] D. Press, T. D. Ladd, B. Zhang, and Y. Yamamoto, Nature (London) **456**, 218 (2008).
[23] J. Mizrahi, B. Neyenhuis, K. G. Johnson, W. C. Campbell, C. Senko, D. Hayes, and C. Monroe, Appl. Phys. B **114**, 45 (2014).
[24] R. Pazourek, S. Nagele, and J. Burgdörfer, Rev. Mod. Phys. **87**, 765 (2015).
[25] R. Santra, V. S. Yakovlev, T. Pfeifer, and Z.-H. Loh, Phys. Rev. A **83**, 033405 (2011).
[26] R. Kronig, J. Opt. Soc. Am. **12**, 547 (1926).
[27] H. A. Kramers, Atti Congr. Int. Fis. **2**, 545 (1927).
[28] R. Kubo, J. Phys. Soc. Jpn. **12**, 570 (1957).
[29] C. W. Peterson and B. W. Knight, J. Opt. Soc. Am. **63**, 1238 (1973).
[30] M. Wu, S. Chen, M. B. Gaarde, and K. J. Schafer, Phys. Rev. A **88**, 043416 (2013).
[31] S. Pabst, A. Sytcheva, A. Moulet, A. Wirth, E. Goulielmakis, and R. Santra, Phys. Rev. A **86**, 063411 (2012).

[32] C. Ott, A. Kaldun, P. Raith, K. Meyer, M. Laux, J. Evers, C. H. Keitel, C. H. Greene, and T. Pfeifer, Science **340**, 716 (2013).
[33] A. Kaldun, C. Ott, A. Blättermann, M. Laux, K. Meyer, T. Ding, A. Fischer, and T. Pfeifer, Phys. Rev. Lett. **112**, 103001 (2014).
[34] H. Mashiko, T. Yamaguchi, K. Oguri, A. Suda, and H. Gotoh, Nat. Commun. **5**, 5599 (2014).
[35] S. R. Leone *et al.*, Nat. Photonics **8**, 162 (2014).
[36] M. B. Gaarde, C. Buth, J. L. Tate, and K. J. Schafer, Phys. Rev. A **83**, 013419 (2011).
[37] Supplemental Material at http://link.aps.org/supplemental/10.1103/PhysRevLett.121.173005 for details about the numerical simulation and the response reconstruction method, which includes Refs. [38–49].
[38] S. I. Themelis, P. Lambropoulos, and M. Meyer, J. Phys. B **37**, 4281 (2004).
[39] J. Feist, S. Nagele, R. Pazourek, E. Persson, B. I. Schneider, L. A. Collins, and J. Burgdörfer, Phys. Rev. A **77**, 043420 (2008).
[40] J. Colgan and M. S. Pindzola, Phys. Rev. Lett. **88**, 173002 (2002).
[41] S. Laulan and H. Bachau, Phys. Rev. A **68**, 013409 (2003).
[42] M. S. Pindzola, J. Phys. B **40**, R39 (2007).
[43] T. N. Rescigno and C. W. McCurdy, Phys. Rev. A **62**, 032706 (2000).
[44] C. W. McCurdy, D. A. Horner, and T. N. Rescigno, Phys. Rev. A **63**, 022711 (2001).
[45] B. I. Schneider and L. A. Collins, J. Non-Cryst. Solids **351**, 1551 (2005).
[46] T. J. Park and J. C. Light, J. Chem. Phys. **85**, 5870 (1986).
[47] E. S. Smyth, Comput. Phys. Commun. **114**, 1 (1998).
[48] C. Ott *et al.*, Nature (London) **516**, 374 (2014).
[49] C. W. McCurdy, M. Baertschy, and T. N. Rescigno, J. Phys. B **37**, R137 (2004).
[50] Z. H. Loh, C. H. Greene, and S. R. Leone, Chem. Phys. **350**, 7 (2008).
[51] W.-C. Chu and C. D. Lin, Phys. Rev. A **82**, 053415 (2010).
[52] W.-C. Chu and C. D. Lin, Phys. Rev. A **85**, 013409 (2012).
[53] W. C. Chu, Phys. Rev. A **84**, 033426 (2011).
[54] K. Meyer, Proc. Natl. Acad. Sci. U.S.A., **112**, 15613 (2015).